Single, two -, and multi-photon driven molecular motion and nanopatterning in azo-polymer films

Zouheir Sekkat[1-5], Hidekazu Ishitobi[5], Mamoru Tanabe[5],
Tsunemi Hiramatsu[5], and Satoshi Kawata[4,5]

[1]Optics and Photonics Center (COP), Moroccan Foundation for Advanced Science & Innovation & Research (MAScIR), Rabat;
[2]University of Rabat, Faculty of Sciences, Department of Chemistry, Rabat-Agdal;
[3]Hassan II Academy of Science and Technology, Rabat, Morocco;
[4]Nanophotonics Laboratory, RIKEN, 2-1 Hirosawa, Wako, Saitama 351-0198, Japan
[5]Department of Applied Physics, Osaka University, Yamada-oka 2-1, Suita, Osaka 565-0871, Japan.

ABSTRACT

We review our work on nanopatterning in azo-polymer films by single, two- and multi-phopton driven molecular motion in solid bulk polymer. It is now known that light induced molecular movement occurs below the polymer glass transition temperature by chromophores photoisomerization via either linear or nonlinear absorption, and in this paper we will show that nanoscale polymer movement is induced by a tightly focused laser beam in an azo-polymer film just at the diffraction limit of light. The deformation pattern which is produced by photoisomerization of the azo dye is strongly dependent on the incident laser polarization and the longitudinal focus position of the laser beam along the optical axis. The anisotropic nanofluidity of the polymer film and the optical gradient force played important roles in the light induced polymer movement. We explored the limits of the size of the photo-induced deformation, and we found that the deformation depends on the laser intensity and the exposure time. The smallest deformation size achieved was 200 nm in full width of half maximum; a value which is nearly equal to the size of the diffraction limited laser spot. Furthermore, a nano protrusion was optically induced on the surface of the films, beyond the limit of light diffraction, by metal tip enhanced near-filed illumination. A silver coated tip was located inside the diffraction limited spot of a focused laser beam (460 nm), and an enhanced near-field, with 30 nm light spot, was generated in the vicinity of the tip due to localized surface plasmons. The incident light intensity was carefully regulated to induce surface nanodeformation by such a near-field spot. A nano protrusion with 47 nm full width of half maximum and 7 nm height was induced. The protrusion occurs because the film is attracted towards the tip end during irradiation. At the top of the protrusion, an anisotropic nanomovement of the polymer occurs in a direction nearly parallel to the polarization of the incident light, and suggests the existence at the tip end of not only a longitudinal, i.e., along the tip long axis, but also a lateral component of the electric field of light. The azo-polymer film helps map the electric field in the close vicinity of the tip. We also report on two-photon patterning of the films. Exposure of azo polymer films, which absorb in the visible range (λ_{max} = 480 nm), to intense 920 nm irradiation leads to polarization dependent patterning which are associated with polymer nanomovement caused by photoselective two-photon cis ↔ trans isomerization, while irradiation at 780 nm induces multi-photon bleaching of the azo chromophore. These wavelengths hit bleaching and isomerization pathways in the chromophore, respectively.

Keywords: Photoisomerization & Photo-orientation; Two- & Multi-photon Absorption; Nonlinear optical polymers; Near-field optics; Nanopatterning; Polymer mass photomechanical movement.

Linear and Nonlinear Optics of Organic Materials XI, edited by Jean-Michel Nunzi,
Rachel Jakubiak, Theodore G. Goodson III, Manfred Eich, Proc. of SPIE Vol. 8113,
81130N · © 2011 SPIE · CCC code: 0277-786X/11/$18 · doi: 10.1117/12.890511

I – INTRODUCTION

Photoinduced patterns of surface deformations in azobenzene containing polymer films have attracted much attention because of possible applications in optical data storage and in micro/nano fabrication, and it is well known that such patterns reflect the state of the incident light polarization and the light intensity distribution [1-5]. Trans ↔ cis photoselective isomerization and molecular reorientation play important roles in the deformation process. Since photoisomerization was shown to enhance molecular mobility far below the glass transition temperature (Tg) of azo-polymers in the beginning of the past decade [6-9], considerable exploration of sub-Tg photo-induced molecular movement was performed especially targeting polymer structural effects, including Tg, the free volume and free volume distribution, the mode of the attachment of the chromophore to a rigid or flexible chain, the molecular weight, and so on [10]. Light induced mass movement in azo polymers, i.e. surface relief gratings (SRGs) [8,9] triggered much studies to understand the mechanism of polymer migration, and most of the studies have focused on SRGs which are fabricated by the interference pattern of two coherent laser beams [11-14]. Yet, there are few reports on surface deformations that are induced by a single focused laser beam [15-17]. To fabricate deformation structures with high spatial resolution, a small irradiation spot is required; a feature which can be achieved by focusing the laser beam by using a high numerical aperture (N.A.) objective lens. In this chapter, we demonstrate patterning of azo-polymer films with a resolution approaching 200 nm by irradiation with a single tightly focused laser beam with a high N.A. objective lens (N.A. = 1.4). We discuss the effect of the incident light polarization and the position of the laser focus on the deformation pattern. In particular, we found that the deformation pattern is strongly dependent on the z- position of the focused laser spot. In addition to the well known trans ↔ cis surface deformation, it will be shown that a gradient force parenting to laser trapping pulls the polymer towards the laser focus. Then we present a systematic study exploring the limits of the size of photo-induced deformation by changing the irradiation intensity and the exposure time. Two-photon patterning of the film samples will also be discussed.

To further reduce the size of the photo-induced surface deformation down to few tens of nanometers, a near-filed optical microscope with an aperture type probe, i.e., tapered optical fiber probe, can be used [18-20]. Near-field optics can confine photons to several tens of nm near the probe tip end and induce nano-scale deformation on the film surface. An apertureless type probe, i.e., metal coated tip which principally generates a smaller light spot than the aperture type probe has also been used [5,21-23]. There are few reports on the mechanism of the near-field surface deformation because efforts were mainly devoted to making smaller fine structures on the surface of polymer films for nano fabrication. Recent reports showed surface deformations that are induced in an azo-polymer film by a combination of optical far- and near-field components of the irradiation light with a high irradiation intensity (typically, 30 KW/cm^2) [4]. In addition, irradiation with high laser intensities bleaches of the azo dyes and produce deformation patterns that are different from those of photo-induced mass movement; a feature which adds complexity to the formation and the understanding of the mechanism of the optical near-field induced surface deformation. In this review, we also report on patterning of azo-polymer films by tip enhanced near-filed, in which the incident laser power was chosen to induce the deformation by the near-field component only, wherein the far-field component had no contribution to the observed surface deformation. We compared the induced deformation patterns with and without tip, and found that a nano protrusion was induced when the tip was inside the laser focus (vide infra). We also found that the deformation pattern was dependent on the incident light polarization, a feature which implies the presence of not only the electric field parallel to the tip axis (Ez) but also the one nearer to incident light polarization (Ex) under the tip end. We will go on to discuss near-field and two-photon nano fabrication.

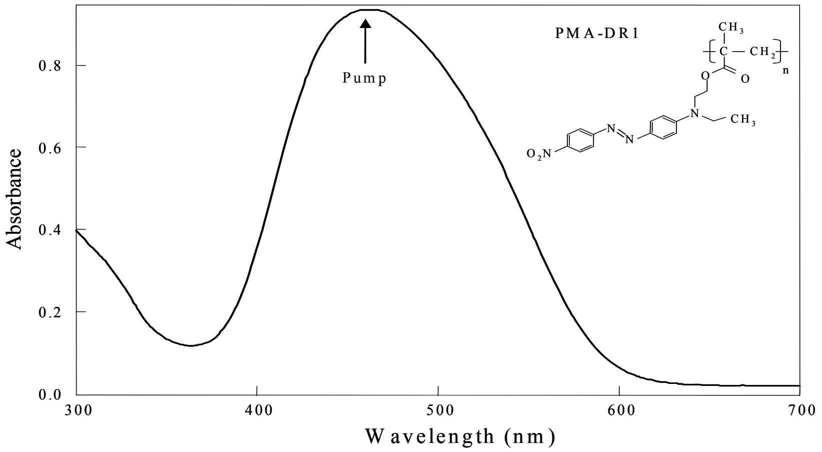

Figure 1: Chemical structure (inset) and absorption spectrum of the trans-DR1-PMA thin film.
The wavelength of excitation is indicated.

II – NANOFABRICATION BY A TIGHTLY FOCUSED LASER BEAM

We prepared 100 nm thin films of poly(Disperse Red 1 methacrylate) (PMA-DR1, product No. 579009, Aldrich; Tg= 82 °C) by spin-casting from a chloroform solution. The remaining solvent was removed by heating the films for an hour at 100 °C. The chemical structure and the absorption spectrum of the film, i.e., trans-DR1 are shown in Fig. 1. Disperse Red 1 (DR1) is a nonlinear optical azo dye which is well known for its trans ↔ cis photoisomerization and for its ability to undergo efficient orientation and trigger important polymer movement when it is excited by polarized light [1]. The orientation effect is due to the highly anisometric nature of its polarizability tensor (rodlike molecule) [24]. The irradiation light source was a linearly polarized 460 nm light from a diode pumped frequency doubled laser (Sapphire 460 LP, Coherent Japan). The wavelength of the irradiation laser corresponds to the maximum absorption band of the film sample. The laser beam was focused by an objective lens (N.A. = 1.4) (Plan Apo 60x, Nikon). The diffraction limited spot diameters in the lateral (X or Y) and longitudinal (Z) axes are ~ 400 nm and 1.0 µm, respectively. Computer controlled piezo stages (P-517 for X and Y axes and P-721 for Z axis, Physik Instruments (PI)) were used to control the position of the focused laser spot in three dimensions. The induced surface deformation of the films was measured by an atomic force microscope (AFM) (SPA-400, SEIKO Instruments Inc.). The AFM was operated in the tapping mode using a Si cantilever to eliminate the mechanical deformation of the films by the cantilever itself.

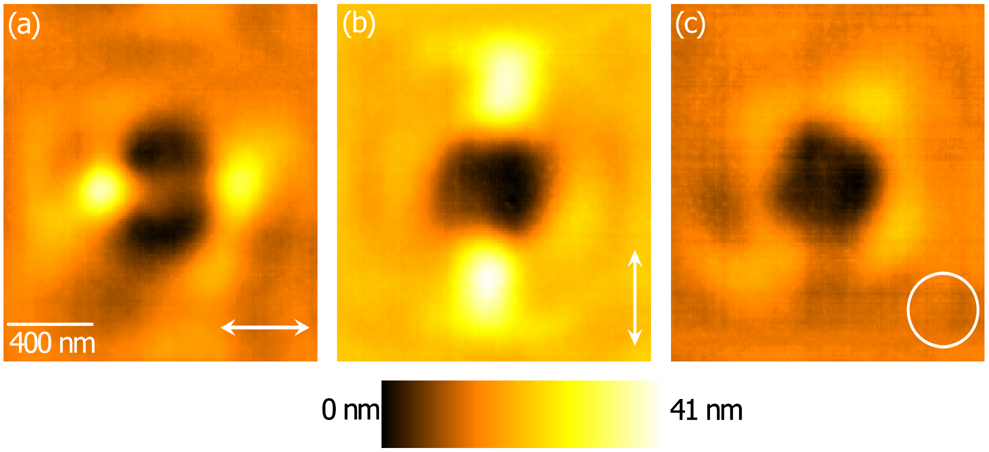

Figure 2: AFM images of the deformation induced by a tightly focused laser beam polarized
(a) horizontally, (b) vertically, and (c) circularly, respectively.

Figure 2 shows AFM images of the surface deformation induced by (a, b) linear and (c) circular polarizations. The polarizations were controlled by half and quarter wave plates. The irradiation intensity and the exposure time were 12.5 mw/cm^2 and 30 s, respectively, and the laser beam was focused on the film surface. Irradiation with linearly polarized light induced the deformation pattern shown in Fig. 2 (a) and (b). It is clearly shown in this figure that the polymer moved along the polarization direction from the centre to the outside of the focused spot, thus producing two side lobes along the polarization direction and a pit at the centre. Indeed this polarization-dependent deformation was confirmed by an experiment in which the polarization direction of the irradiation light was rotated through an angle of 90 degrees and the induced pattern followed the polarization of the light (see Fig. 2 (a) versus (b)). In contrast to irradiation with linear polarization, irradiation with circularly polarized light induced a deformation pattern in which the polymer moved from the centre to the outside of the focused laser spot, thus forming a doughnut shape pattern (Fig. 2 (c)). For both linear and circular polarizations, the polymer migrates in the direction of the light gradient from high to low light intensity regions, and the polarization dependence demonstrates that the light-induced polymer movement is anisotropically photo-fluidic [5].

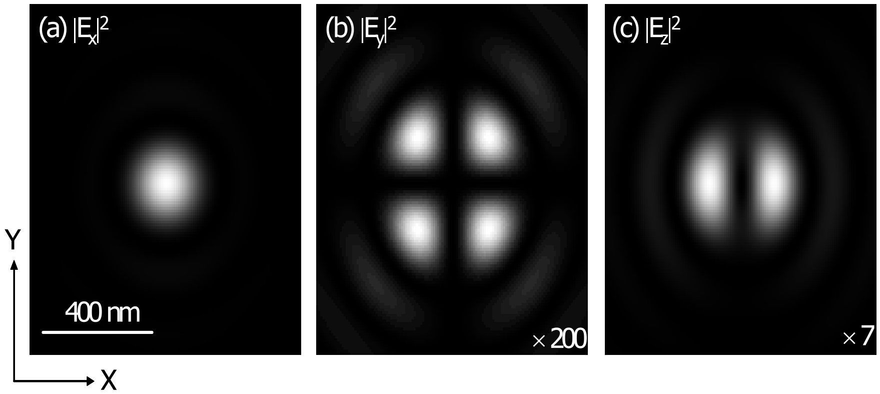

Figure 3: Calculated distributions of squared electric field components created by a tightly focused linearly polarized laser beam. The each components of electric field of (a) Ex, (b) Ey, and (c) Ez are shown. The polarization direction is X, Z is perpendicular to the film, and Y is perpendicular to both X and Z. The distribution was calculated assuming a refractive index of the surrounding medium equal to 1.5.

The observed polarization dependence is consistent with the one obtained after irradiation with a low N.A. lens [15]. When a laser beam is tightly focused by a high N.A. objective lens, a non negligible electric field E_z component is created along the optical axis. The intensity distributions corresponding to E_x, E_y, and E_z at the focal position are different, and shown in Fig. 3, and they should lead to different deformation patterns. However, in our experimental conditions, only E_x contributes appreciably to the deformation. With N.A. = 1.4 and wavelength = 460 nm, the maximum intensity corresponding to E_z and E_y are 7 and 200 times smaller than that of E_x, respectively.

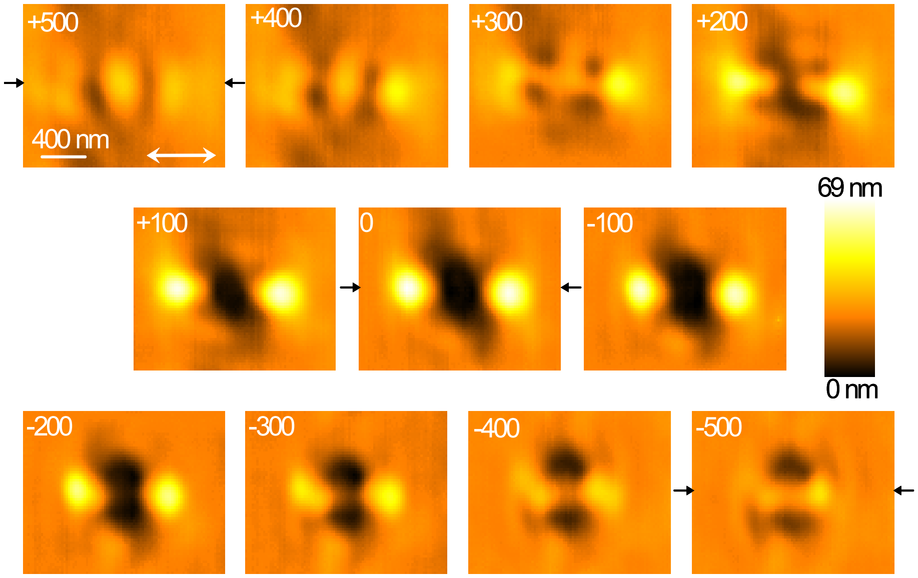

Figure 4: AFM images of the surface deformation induced by changing the Z-position of the focused laser spot. The Z-position was varied from -500 nm to +500 nm with an interval of 100 nm. The values inside each figure represent the Z-position of the focus (unit is nm). The polarization direction is indicated.

Figure 4 shows AFM images of the photo-induced deformation which have been obtained by changing the Z-position of the focused laser spot. The Z-position was controlled by the z-axis piezo stage which was attached to the objective lens. The irradiation started 500 nm under the film surface (Z = -500 nm), then the Z-position was moved to upper positions with an interval of 100 nm, and the next irradiation was done at a different lateral (X-Y) position. This procedure was repeated until the Z-position reached 500 nm upper the film surface (Z = +500 nm). For each irradiation, the irradiation intensity and the exposure time were 12.5 mw/cm^2 and 60 s, respectively.

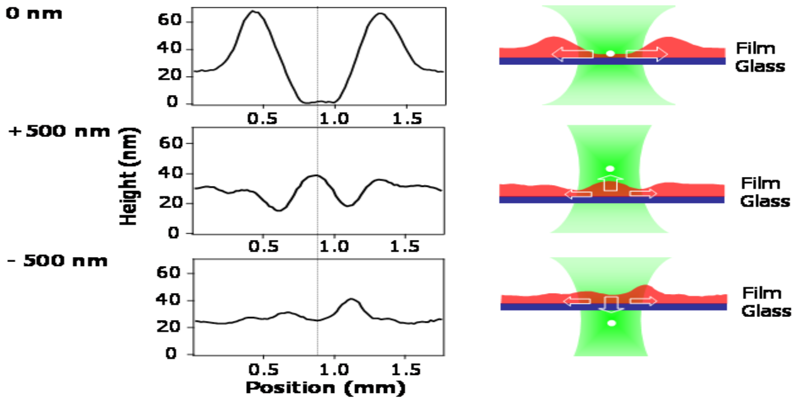

Figure 5: (Left column) Line plots of the surface deformation at (a) Z = +500 nm, (b) Z = 0 nm, and (c) Z = -500 nm. The positions of the each plot correspond to the directions which are between the arrows indicated in Fig. 4. (Right column) Schematics describing the relationship between the Z-position of the focus and the film surface. The arrows oriented laterally and longitudinally in these schematics indicate the direction of the anisotropic photo-fluidity and the optical gradient force, respectively.

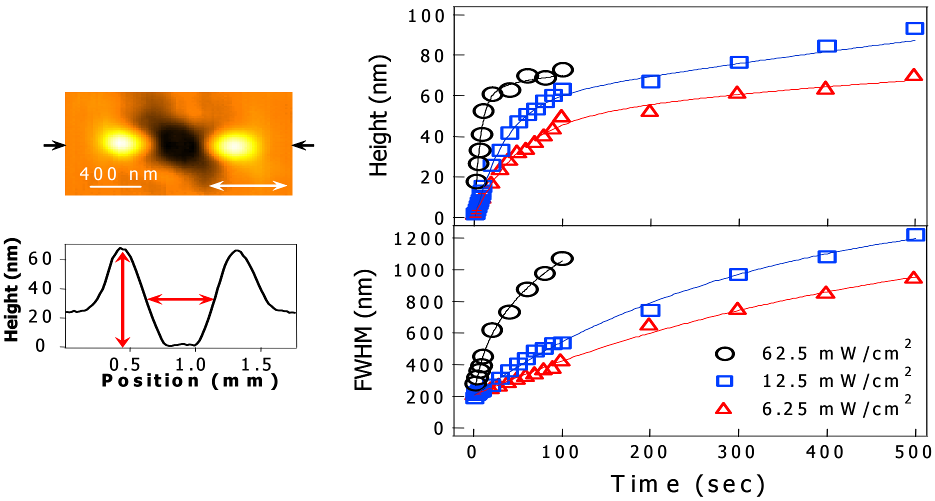

Figure 6: Size dependence of the surface deformation on the irradiation intensity and the exposure time. A typical deformation pattern and the corresponding line pot are shown in the left of the figure and the definitions of the height and FWHM are indicated. Scatters are experimental data, and solid lines are exponential empirical theoretical fits.

When the Z-position was just on the film surface (Z = 0 nm), the deformation pattern was the same as the one shown in Fig 2 (a) or (b). It is interesting to note that at distances larger than 200 nm above the film surface in air, the polymer formed a protrusion coming out towards the center of the laser focus and suggesting the existence of a gradient force [25] that pulls the polymer towards the region of maximum intensity (see Fig. 5). This is optical trapping of a viscoelastic polymer showing nanoelasticity over 20 nm; i.e. the maximum height of the protrusion obtained at z= + 500 nm. For distances between 200 and 0 nm, the overlap of the laser intensity and the film are large enough to produce dips at the center as explained above. When the laser is focused into the glass substrate, there is no protrusion formed, because the polymer movement is blocked by the substrate. In a systematic set of experiments, we studied the dependence of the size of the photo-induced deformation on the intensity of the irradiation light and the exposure time. In those experiments, the irradiation light is linearly polarized and focused by a 1.4 N.A. objective lens. The deformation pattern was studied just at the laser focus, i.e. Z = 0 nm, for three irradiation intensities (6.25, 12.5, 62.5 mW/cm^{2}), and exposure times according to the series 1 to 500 s for 6.25 and 12.5 mW/cm^{2}, and 1 to 100 s for 62.5 mW/cm^{2}. The deformation patterns obtained at all intensities at all times of irradiation were the same, but the size of the deformation was different. Figure 6 shows the dependence of the height and the full width at half maximum (FWHM) of deformation pattern along the direction parallel to the light polarization on the irradiation intensity and the exposure time. The height is defined as the difference between the top of the side lobes and the bottom of the central pit as shown in Fig. 6. As is can be seen as well from this figure, the rate of the deformation of the height and FWHM decreased with the increasing irradiation dose, and the higher the irradiation intensity, the faster the increase of both the height and FWHM. The height increases more rapidly than FWHM which needs more time to reach saturation. The height increases rapidly at small irradiation doses, and saturates at larger irradiation doses near 90 nm, a value which corresponds to the film thickness. The minimum FWHM of the fabricated pattern is about 200 nm; a value which corresponds to the size of the diffraction limited laser spot.

III – NEAR-FIELD NANOFABRICATION BEYOND THE DIFFRACTION LIMIT OF LIGHT

We prepared 50 nm thin films of PMA-DR1 as explained in section II, and the irradiation light source and the focused beam were as explained in section II as well. An atomic force microscope (AFM) tip (Silicon Cantilever CSG01, NT-MDT) was covered by silver with a vacuum evaporator. The diameter of the tip end was found to be 30 nm by using a scanning electron microscope (see Fig. 7). The tip was approached to the diffraction limited focused spot on the film by an AFM (Bioprobe, Park Scientific Instruments) operating in a contact mode, and the enhanced near-field with a 30 nm diameter spot was generated in the vicinity of the tip via localized surface plasmons (see schematic in Fig. 8). In this configuration, the tip was permanently in contact with the film surface. The irradiation light intensity was 3 mW/cm^2 (versus 30 KW/cm^2 in reference [4]). As explained in the previous section, a computer controlled piezo stage was used to control the position of the laser spot, and the induced pattern was observed by an AFM which was operating in the tapping mode.

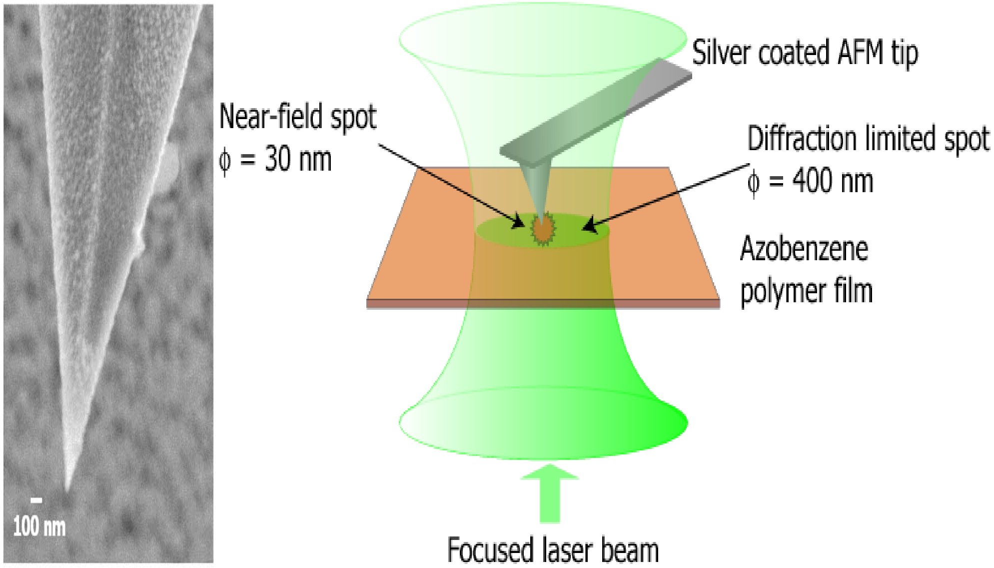

Figure 7: (Left) SEM image of the silver coated AFM tip. (Right) Schematic of the near-field surface deformation configuration.

Figure 8 shows the AFM image of the surface deformation which was induced with and without the silver coated tip. The irradiation intensity and the exposure time were 3 mW/cm^2 and 10 s, respectively; an irradiation dose which permitted fabrication by only the near field component of the light (vide infra). It can be clearly seen from Fig. 8 that the protrusion was induced only with the tip present inside the focused spot, and no deformation was induced when the tip was away from it. The height of the protrusion was found to be 7 nm, and the lateral size was less than the diffraction limited spot size, indicating that the surface deformation was induced by only the near-field component of the light.

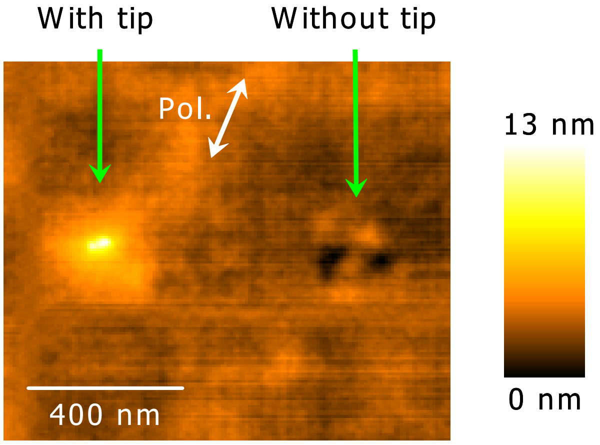

Figure 8: AFM image of the surface deformation induced by irradiation with and without the silver coated AFM tip. The polarization direction and the scale bar are indicated.

It is well known that the component of the electric field parallel to the tip axis (E_z) is effectively enhanced near the tip end due to the local surface plasmons [26]. The polymer under the tip is pulled by the optical gradient force which is generated by E_z [25, 27] and formed the nano protrusion. This finding is in good agreement with the experimental results which were recently reported by us, in which we studied nanoscale polymer movement induced by a tightly focused laser beam, and we found that the deformation pattern was strongly dependent on the longitudinal focus position of the laser beam along the optical axis whereby the film is pulled by the optical gradient force, which is due to the focused beam, towards the focus when the beam is focused in air just on top of the sample surface [28]. In the present optical set up, the nano light spot was placed just onto the film surface, and it was kept on it while the protrusion was being formed during irradiation. Here too, the film was pulled by the optical gradient force towards the nanosource of light; e.g. the tip end, much like the case of a tightly focused beam on top of the film (vide infra). The field enhancement effect due to the metal tip allowed for the fabrication of near-field surface features with a light intensity which is as low as 3 mW/cm^2.

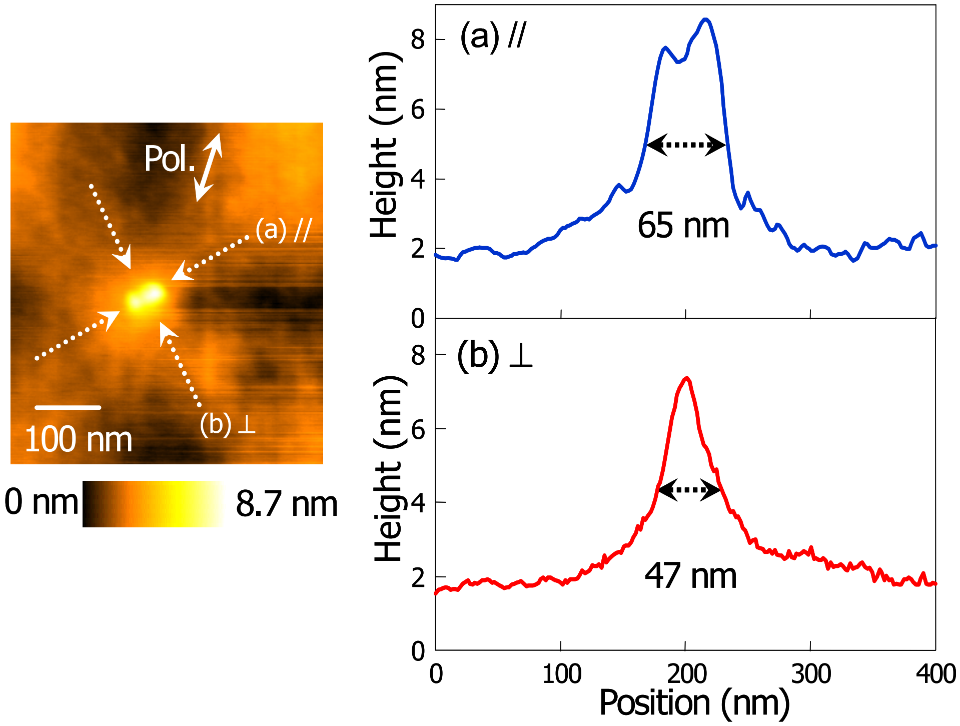

Figure 9: AFM image of the near-field surface deformation (expanded view of the left side of the Fig. 8).
The polarization direction and the scale bar are indicated. (a) and (b) show the line profiles in the directions near parallel and near perpendicular to the incident light polarization, respectively.
The FWHMs of the surface deformation in the parallel and perpendicular directions are also indicated.

Figure 9 shows an expanded view of the surface deformation induced by the near-field irradiation (left side of Fig. 8). It is found that the long axis of the deformation pattern was along a direction which is, not quite, but near the parallel to the incident light polarization. This uniaxial anisotropic polymer movement suggests that the polymer moved along the polarization direction. The full width of half maximum of the protrusion was found to be 65 and 47 nm in the direction nearly parallel (//) and perpendicular (□) to the incident light polarization, respectively. Here too, the anisotropic photo-fluidity of the polymer tends to induce a polymer mass movement in the direction parallel to the incident light polarization [5, 27]. This anisotropic polymer movement implies the presence under the tip end of a component of the electric field which is near the parallel to the polarization direction [29]. The azo-polymer helps map the electric field just at the tip apex.

In fact, the fabricated feature which is due to Ex is much smaller than the one due to Ez and it confirms the well known phenomenon that only the longitudinal component Ez drives efficient oscillations of the surface plasmons polaritons at the metal tip and leads to a strong field enhancement, i.e., enhancement of Ez, at the tip apex [26]. Two-photon patterning of azo-polymers is discussed next.

IV – TWO-PHOTON PATTERNING

Recently, two-photon isomerization and reorientation of azo dyes in polymers have attracted much attention because of the scientific and technological extension into nanophotonics [30-46]. Basically, the photoreaction can be induced by tightly focused lasers into confined volumes - a resolution of 120 nm has been achieved for three dimensional nanofabrication in photopolymerizable resins [47] -, and novel scientific information may be obtained, especially with regard to one versus two- or multi-photon reaction pathways – the one and two-photon transition dipole moments of a diarylethene derivative have been found to be perpendicular to each other in two-photon isomerization experiments [30]. In, this review, we show that azo-polymer films, are patterned by two-photon isomerization as well [48], and we discuss the effect of the incident light polarization and the position of the laser focus (Z-position of the focus) on the deformation patterns induced by two-photon absorption. We discuss the mechanism of the induced surface deformation for two-photon versus one-photon absorption. The effect of photobleaching is also discussed by studying the effect of the irradiation wavelength, i.e., 780 nm versus 920 nm irradiation, on the induced patterns.

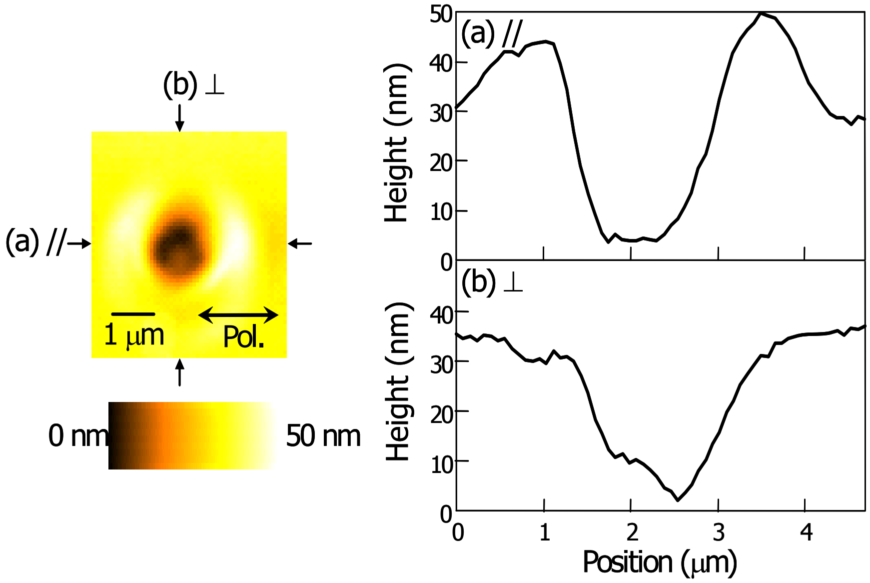

Figure 10: AFM images of the deformation induced at 920 nm light when Z-position of the focused laser spot is + 2 μm. The polarization direction is indicated by the arrow. The line plots (a) parallel and (b) perpendicular to light polarization are shown. The positions of the each plot correspond to the directions that are between the arrows indicated.

We prepared 150 nm thin films of PMA-DR1 by spin coating as explained earlier. The films were irradiated by a linearly polarized near infrared light from a Ti:Sapphire laser (Spectral Physics, Mai Tai, pulse width = 130 fs; repetition rate = 80 MHz) to induce patterns via a two-photon absorption process. The laser light was focused by an objective lens (N.A. = 0.55) from the bottom of a cover glass. The diffraction limited spot diameter in the lateral and longitudinal axes are 2 μm and 12 μm, respectively. A computer controlled piezo stage (Melles Griot, Nanoblock), on which the sample was placed, was used to control the position of the irradiation spot with respect to the sample surface. The surface topology of the deformed films was measured by an atomic force microscope (AFM) (SEIKO Instruments Inc., SPA-400). The AFM was operated in the tapping mode.

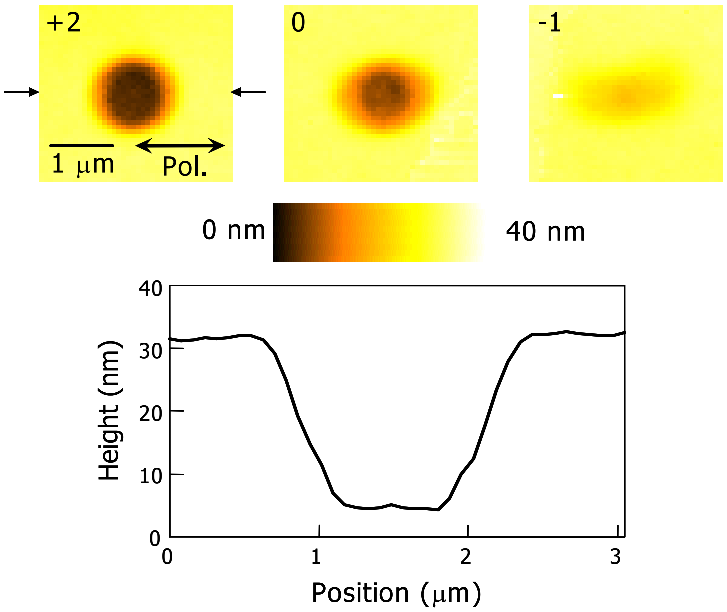

Figure 11: (Upper row) AFM images of the surface deformation induced at 780 nm light by changing the Z-position of the focused laser spot. The Z-position was varied from -5 µm to +5 µm with an interval of 1 µm. Only images at +2 µm, 0 µm, -1 µm are shown. The values inside each figure represent the z-position of the focus (unit is µm). The polarization direction is indicated by the arrow. (Lower row) Line plots of the surface deformations at Z = +2 µm. The position of the plot corresponds to the directions that are between the arrows indicated.

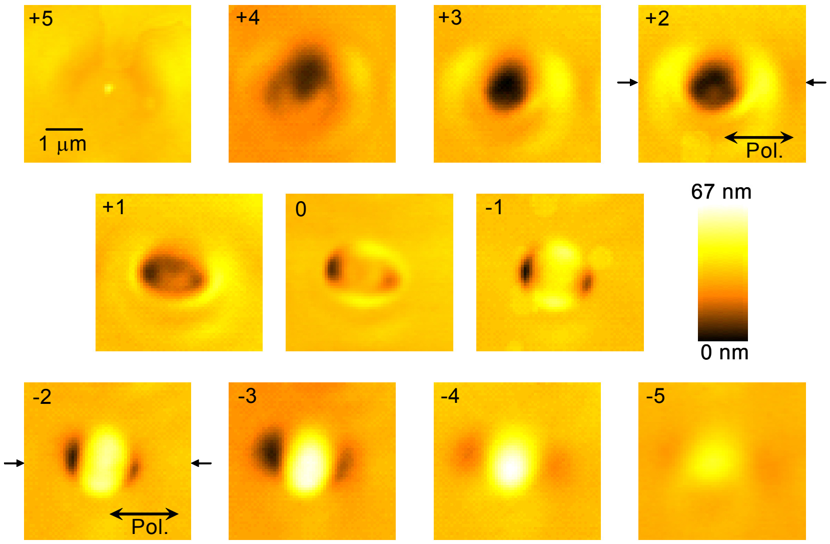

Figure 12: AFM images of the surface deformation induced at 920 nm light by changing the Z-position of the focused laser spot. The Z-position was varied from -5 µm to +5 µm with an interval of 1 µm. The values inside each figure represent the Z-position of the focus (unit is µm). The polarization direction is indicated by an arrow.

Figure 10 shows an AFM image of the surface deformation induced by a focused, linearly polarized, 920 nm irradiation (irradiation intensity = 61 kW/cm^2; and exposure time = 60 s). This figure corresponds to a spot center 2 µm above the film surface in air. A similar behavior is observed when the center of the spot is 1 µm above and just at the film surface *(vide infra)*. It can be clearly seen from this figure that the polymer moves along the polarization direction from the center to the outside of the focused spot, thus producing two side lobes along the polarization direction and a pit at the center. This can also be seen at the AFM topographic line scans along and perpendicular to the direction of light polarization. This observed behavior, which is due to a photonic effect, i.e., polarization dependent, and not to heat deposition, is much like that observed with single photon isomerization (vide infra). At half the 920 nm fundamental wavelength, i.e., 460 nm, the sample presents a strong absorption suggesting that two-photon isomerization is at the origin of the surface deformation.

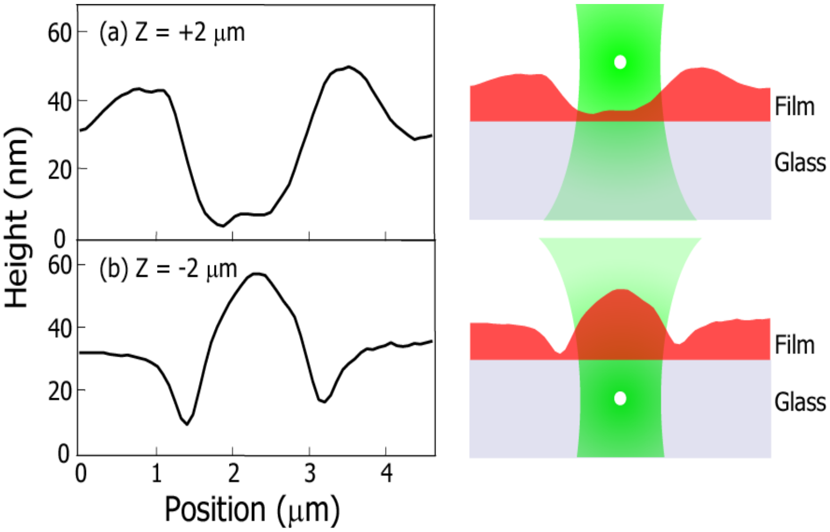

Figure 13: (Left column) Line plots of the surface deformations at (a) Z = +2 μm and (b) Z = -2 μm. The positions of the each plot correspond to the directions that are between the arrows indicated in Fig. 12. (Right column) Schematics describing the relationship between the Z-position of the focus and the film surface.

The effect of dye photobleaching on the induced patterns was investigated by changing the irradiation wavelength of the laser light to 780 nm to confirm that the surface patterns induced by 920 nm irradiation were in fact due to two-photon isomerization and not to bleaching of the dye. Indeed, in a recent report, we showed that DR1 undergoes bleaching under irradiation at 780 nm, at the same range of light intensity, i.e., GW/cm^2, via a multi-photon absorption process [33]. Furthermore, Fig. 11 shows that the surface deformation induced by 780 nm irradiation at the same light intensity as that of 920 nm irradiation formed dips at the center of focus, and the patterns are independent from the incident light polarization. The same behavior was observed for all Z-positions of the focus. Only those at + 2 μm, and at the film surface, i.e., 0 μm, and - 1 μm are shown, and no deformation was observed when the Z-positions of the spot was smaller than – 2 μm. This finding confirms that the surface deformations shown on Fig. 13 were induced by multi-photon bleaching of DR1. Note that while an ablated polymer surface by a high intensity pulsed laser looks rough under AFM imaging, due to the deposition of fragments of the ablated polymer at the film surface [49], the AFM images of Fig. 11 are smooth outside the irradiated area and reinforce photobleaching versus ablation as a mechanism of the dip formation.

Figure 12 shows AFM images of the photo-induced patterns observed by changing the Z-position of the focused laser spot with irradiation at 920 nm. This irradiation, as well as that done at 780 nm which is discussed in the previous paragraph, started 5 μm above the film surface (Z = +5 μm) in air, then the Z-position was moved to lower positions, i.e., towards the film, with an interval of 1 μm, and the next irradiation was done at a different lateral (X-Y) position. This procedure was repeated until the Z-position reached -5 μm (Z = -5 μm), i.e., in the other side of the film, inside the glass slide. For each irradiation, the irradiation intensity and the exposure time were 61 kW/cm^2 (peak intensity = 5.9 GW/cm^2) and 60 s, respectively.

Fig. 12 shows that when the Z-position of the focus is above the film surface in air (Z > 0 μm), the polymer moved along the polarization direction from the center to the outside of the focused spot, thus producing two side lobes along the polarization direction and a pit at the center *(vide supra)*. A somewhat contrasted behavior is observed when the Z-position of the focus is below the film surface (Z < 0 μm), i.e., the polymer moves from the outside to the center of the focused laser spot always along the direction of the polarization of the excitation light and formed a protrusion at the center and two dips, one at each side of the protrusion along the polarization direction (see also Fig. 13). When the distance between the focus and sample surface is larger than 5 μm (Z > 5 μm, Z < -5 μm), no deformation is induced because the intensity of the light spot at the film is not large enough to induce a pattern.

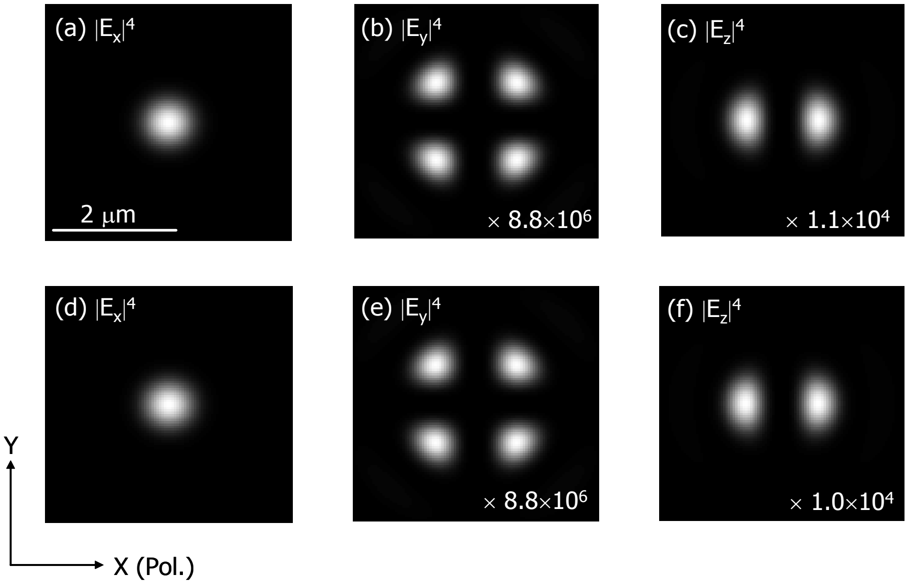

Figure 14: Calculated field distributions of 4th power of electric field components created by a focused linearly polarized laser beam in the presence of the interface between air (n = 1.0) and polymer (n = 1.5). The distributions were calculated in a XY in-plane which is located at 5 nm below the interface. The upper and lower figures show the field distributions when the Z-position of the focus is +2 μm and -2 μm, respectively. Each components of electric field of (a,d) Ex, (b,e) Ey, and (c,f) Ez are shown. The polarization direction is X, and Z is perpendicular to the film surface, and Y is perpendicular to both X and Z.

At a low N.A. objective lens, i.e., N.A. = 0.55 in the present experiments, the dominant component of electric field at the focus is the one along the polarization direction (Ex) when the incident light is linearly polarized along X. Indeed, electromagnetic calculations that we performed for the intensity distribution at 5 nm below the air (n = 1.0) / polymer (n = 1.5) interface when the beam focus is at + 2 μm and - 2 μm, show that the Y and Z components of the fourth power of the optical field are 4 and 5 orders of magnitude smaller that the fourth power of Ex, respectively (see Fig. 16). So, during two-photon patterning, polymer movement proceeds in the direction of the light polarization (X) *(vide supra)*.

Figure 14 also shows that the field distribution is nearly unchanged when the z-position of the focus is at +2 μm (in air) and -2 μm (in the cover glass). Since the field distribution in X-Y plane is quasi-identical from both sides of the polymer film, i.e., the laser is independently focused at the same distance from the film in air and glass, the presence of an intensity gradient along the Z axis leads to the formation of the observed deformation. Note that when the same experiments were performed with one-photon absorption at 460 nm on the same polymer (see e.g. section II), an optical gradient force, which is proportional to the Z-intensity gradient, was observed to be attractive, i.e., a protrusion was formed when the focus was in the air and not in the glass. It is interesting to note that this behavior is opposite to that observed with two-photon isomerization. We do not have yet a clear explanation for this phenomenon, and more experiments are necessary in order to assess how the intensity gradient contributes to the formation of the patterns induced by one and two-photon isomerization. Systematic studies on irradiation wavelength and doses and so on are also needed in order to clarify the mechanism of the formation of the patterns, as well as for assessing the limit of the spatial resolution of two-photon surface nanofabrication on azo-polymers by a single tightly focused laser, especially at a high N.A. objective lens.

V - CONCLUSION

Both one- and two-photon absorption induce isomerization and patterns in azo-polymers. In both one and two-photon cases, the polymer moves in the direction of the irradiation light polarization. We also found that the induced surface pattern strongly depends on the Z-position of the laser focus suggesting a contribution, to the observed patterns, of a light intensity gradient along the Z-axis, i.e., the direction of the propagation of the laser. We showed that nanomovement of photosensitive polymers occurs by polarization sensitive photoisomerization in a nanoscale, and we studied polymer nanomovement induced by a tightly focused laser beam and a metal tip enhanced near-field irradiation. In particular, we observed a patterns which is induced only by the near-field component of the light with a resolution beyond the diffraction limit of light by controlling the irradiation light intensity. The optical gradient force which is generated by a strong Ez pulls the polymer towards the tip end, and anisotropic nanofluidity generated by the relatively small Ex moves the polymer along the polarization direction in the film plane. Future works of near-field nano fabrication on azo-polymers should focus on systematic studies at different irradiation doses and polarization states and irradiation configurations with respect to the tip axis. Additional experimental and theoretical studies are needed to assess the contribution of the light intensity gradient and radiation forces and torques to the formation of patterns by one and two-photon isomerization [50-54].

REFERENCES

[1] Z. Sekkat, W. Knoll, *Photoreactive Organic Thin Films* (Academic Press, USA, 2002).

[2] K. Koyayashi, C. Egami and Y. Kawata, "Optical Storage Media with Dye-Doped Minute Sphere on Polymer Films," Opt. Rev. **10**, 262-266 (2003).

[3] C. Hubert, A. Rumyantseva, G. Lerondel, J. Grand, S. Kostcheev, L. Billot, A. Vial, R. Bachelot, P. Royer, S-H Chang, S. K. Gray, G. P. Wiederrecht, and G. C. Schatz, "Near-Field Photochemical Imaging of Nobel Metal Nanostructures," Nano Lett. **5**, 615-619 (2005).

[4] Y. Gilbert, R. Bachelot, A. Vial, G. Lerondel, P. Royer, A. Bouhelier, and G. P. Wiederrecht, "Photoresponsive polymers for topographic simulation of the optical near-field of a nanometer sized gold tip in a highly focused laser beam," Opt. Express **13**, 3619-3624 (2005).

[5] P. Karageorgiev, D. Neher, B. Schulz, B. Stiller, U. Pietsch, M. Giersig, and L. Brehmer, "From anisotropic photo-fluidity towards nanomanipulation in the optical near-field," Nature Materials **4**, 699-703 (2005).

[6] Z. Sekkat and M. Dumont, "Photoassisted Poling of Azo Dye Deped Polymeric Films at Room Temperature," Appl. Phys. B **54**, 486-489 (1992).

[7] F. Charra, F. Kajzar, J. M. Nunzi, P. Raimond, and E. Idiart, "Light-induced second-harmonic generation in azo-dye polymers," Opt. Lett. **18**, 941-943 (1993).

[8] P. Rochon, E. Batalla, and A. Natansohn, "Optically induced surface gratings on azoaromatic polymer films," Appl. Phys. Lett. **66**, 136-138 (1995).

[9] D. Y. Kim, S. K. Tripathy, L. Li, and J. Kumar, "Laser-induced holographic surface relief gratings on nonlinear optical polymer films," Appl. Phys. Lett. **66**, 1166-1168 (1995).

[10] Z. Sekkat, D. Yasumatsu, and S. Kawata, "Pure Photoorientation of Azo Dye in Polyurethanes and Quantification of Orientation of Spectrally Overlapping Isomers," J. Phys. Chem. B **106**, 12407-12417 (2002)

[11] P. Lefin, C. Fiorini, J. M. Nunzi, "Anisotropy of the photoinduced translation diffusion of azo-dyes," Opt. Mater. **9**, 323-328 (1998).

[12] F. L. Labarthet, J. L. Bruneel, T. Buffeteau, and C. Sourisseau, "Chromophore Orientations upon Irradiation in Gratings Inscribed on Azo-Dye Polymer Films: A Combined AFM and Confocal Raman Microscopic Study," J. Phys. Chem. B **108**, 6949 (2004).

[13] A. Natansohn and P. Rochon, "Photoinduced Motions in Azobenzene-Based Polymers," Chapter 13 in ref. [1], 400-423, and references therein.

[14] O. N. Oliveira, L. Li, J. Kumar, and S. Tripathy, "Surface-Relief Gratings on Azobenzene-Containing Films," Chapter 14 in ref. [1], 430-480, and references therein.

[15] S. Bian, J. M. Williams, D. Y. Kim, L. Lin, S. Balasubramanian, J. Kumar and S. Tripathy, "Photoinduced surface deformations on azobenzene polymer films," J. Appl. Phys. **86**, 4498-4508 (1999).

[16] Y. Gilbert, R. Bachelot, P. Royer, A. Bouhelier, G. P. Wiederrecht, and L Novotny, "Longitudinal anisotropy of he photoinduced molecular migration in azobenzene polymer films," Opt. Lett. **31**, 613-615 (2006).

[17] T. Grosjean and D Courjon, "Photopolymers as vectorial sensors of the electric field," Opt. Express **14**, 2203-2210 (2006).

[18] S. Davy and M. Spajer, "Near filed optics: Snapshot of the field emitted by a nanosource using a photosensitive polymer," Appl. Phys. Lett. **69**, 3306-3308 (1996).

[19] T. Fukuda, K. Sumaru, T. Kimura, H. Matsuda, Y. Narita, T. Inoue, and F. Sato, "Observation of Optical Near-Field as Photo-Induced Surface Relief Formation," Jpn. J. Appl. Phys. **40**, L900-L902 (2001).

[20] S. Patanè, A. Arena, M. Allegrini, L. Andreozzi, M. Faetti, and M. Giordano, "Near-field optical writing on azo-polymethacrylate spin-coated films," Opt. Commun. **210**, 37-41 (2002).

[21] F. Iwata, K. Kobayashi, A. Sasaki, Y. Kawata, C. Egami, O. Sugihara, M. Tuchimori and O. Watanabe, "Nanometre-scale modification of a urethane-urea copolymer film using local field enhancement at an apex of a metal coated probe," Nanotechnology **13**, 138-142 (2002).

[22] R. Bachelot, F. H'Dhili, D. Barchiesi, G. Lerondel, R. Fikri, P. Royer, N. Landraud, J. Peretti, F. Chaput G. Lampel, J-P. Boilot, and K. Lahlil, "Apertureless near-field optical microscopy: A study of the local tip field enhancement using photosensitive azobenzene-containing films," J. Appl. Phys. **94**, 2060-2072 (2003).

[23] Y. Gillbert, R. Fikri, A. Ruymantseva, G. Lerondel, R. Bachelot, D. Barchiesi, and P. Royer, "High-resolution nanophotolithography in atomic force microscopy contact mode," Macromolecules **37**, 3780-3791 (2004).

[24] Z. Sekkat, J. Wood, W. Knoll, W. Volksen, R. D. Miller, "Light-induced orientation in a high glass transition temperature polyimide with polar azo dyes in the side chain," J. Opt. Soc. Am. B **13**, 1713-1724 (1996).

[25] A. Ashkin, J. M. Dziedzic, J. E. Bjorkholm, and S. Chu, "Observation of a single-beam gradient force optical trap for dielectric particles," Opt. Lett. **11**, 288-290 (1986).

[26] Y. Inouye, and S. Kawata, "Near-field scanning optical microscope with a metallic probe tip," Opt. Lett. **19**, 159-161 (1994).

[27] L. Novotny, R. X. Bian, and X. S. Xie, "Theory of Nanometric Optical Tweezers," Phys. Rev. Lett. **79**, 645-648 (1997).

[28] H. Ishitobi, M. Tanabe, Z. Sekkat and S. Kawata, "The anisotropic nanomevement of azo-plymers," Opt. Express **15**, 652-659 (2007).

[29] H. Ishitobi, M. Tanabe, Z. Sekkat and S. Kawata, "Nanomovement of azo polymers induced by metal tip enhanced near-field irradiation," Appl. Phys. Lett. **91**, 091911 (2007).

[30] Z. Sekkat, H. Ishitobi, and S. Kawata, "Two-photon isomerization and orientation of photoisomers in thin films of polymer," Opt. Commun. **222**, 269-276 (2003).

[31] Z. Sekkat, "Isomeric orientation by two-photon excitation: a theoretical study," Opt. Commun. **229**, 291-303 (2004).

[32] H. Ishitobi, Z. Sekkat, and S. Kawata, "Ordering of azobenzenes by two-photon isomerization," J. Chem. Phys. **125**, 164718 (2006).

[33] H. Ishitobi, Z. Sekkat, and S. Kawata, "Photo-orientation by multiphoton photoselection," J. Opt. Soc. Am B **23**, 868-873 (2006).

[34] M. Maeda, H. Ishitobi, Z. Sekkat and S. Kawata, "Polarization storage by nonlinear orientational hole burning in azo dye-containing polymer films," Appl. Phys. Lett. **85**, 351-353 (2004).

[35] X. Li, J.W.M. Chon, R.A. Evans, and M. Gu, "Two-photon energy transfer enhanced three-dimensional optical memory in quantum-dot and azo-dye doped polymers," Appl. Phys. Lett. **92**, 063309 (2008).

[36] D. Gindre, I. Ka, A. Boeglin, A. Fort, and K.D. Dorkenoo, "Image storage through gray-scale

encoding of second harmonic signals in azo-dye copolymers" Appl. Phys. Lett. **90**, 094103 (2007).

[37] D. Gindre, A. Boeglin, A. Fort, L. Mager, and K.D. Dorkenoo, "Rewritable optical data storage in azobenzene copolymers" Opt. Express **14**, 9896-9901 (2006).

[38] D. Gindre, A. Boeglin, G. Taupier, O. Crégut, J.-P. Vola, A. Barsella, L. Mager, A. Fort, and K.D. Dorkenoo, "Toward submicrometer optical storage through controlled molecular disorder in azo-dye copolymer films," J. Opt. Soc. Am. B **24**, 532-537 (2007).

[39] C.R. Mendonça, U.M. Neves, L. De Boni, A.A. Andrade, D.S. dos Santos Jr., F.J. Pavinatto, S.C. Zilio, L. Misoguti, O.N. Oliveira Jr, "Two-photon induced anisotropy in PMMA film doped with Disperse Red 13," Opt. Commun. **273**, 435-440 (2007).

[40] S. Liu, K.S. Lin, V.M. Churikov, Y.Z. Su, J.T. Lin, T.-H. Huang, and C.C. Hsu, "Two-photon absorption properties of star-shaped molecules containing peripheral diarylthienylamines," Chem. Phys. Lett. **390**, 433-439 (2004).

[41] N.D. Lai, W.L. Wang, J.H. Lin, and C.C. Hsu, "Optical manipulation of third-harmonic generation via either one- or two-photon excitation in diarylethene-polymethylmethacrylate polymer thin films," Appl. Phys. B **80**, 569-572 (2005).

[42] S.W. Magennis, F.S. Mackay, A.C. Jones, K.M. Tait, and P.J. Sadler, "Two-Photon-Induced Photoisomerization of an Azo Dye," Chem. Mater. B **17**, 2059-2062 (2005).

[43] C.C. Corredor, K.D. Belfield, M.V. Bondar, O.V. Przhonska, F.E. Hernandez, and O.D. Kachkovsky, "One- and two-photon photochromism of 3,4-bis-(2,4,5-trimethyl-thiophen-3-yl)furan-2,5-dione," J. Photochem. Photobio. A **184**, 177-183 (2006).

[44] Y. Jung, V.M. Kozenkov, S.A. Magnitskii, and N.M. Nagorskii, "Optical orientation of azo dye molecules in a thin solid film upon nonlinear excitation by femtosecond laser pulses," Quantum Electronics **36**, 1056-1057 (2006).

[45] K.D. Belfield, M.V. Bonder, C.C. Corredor, F.E. Hernandez, O.V. Przhonska, and S. Yao, "Two-Photon Photochromism of a Diarylethene Enhanced by Förster Resonance Energy Transfer form Two-Photon Absorbing Fluorenes," ChemPhysChem **7**, 2514-2519 (2006).

[46] A.M. Dubrovkin, Y. Jung, V.M. Kozenkov, S.A. Magnitskii, and N.M. Nagorskiy, "Nonlinear induce polarization dependent scattering in solid state azo-dye films," Laser Phys. Lett. **4**, 275-278 (2007).

[47] S. Kawata, H.-B. Sun, T. Tanaka, and K. Takada, "Finer features for functional microdevices - Micromachines can be created with higher resolution using two-photon absorption," Nature **412**, 697-698 (2001).

[48] H. Ishitobi, S. Shoji, T. Hiramatsu, H.-B. Sun, Z. Sekkat, and S. Kawata,"Two-photon induced polymer nanomovement" Optics Express **16(18)**, 14106-14114 (2008).

[49] H. Hisakuni and K. Tanaka, "Optical microfabrication of chalcogenide glasses," Science **270**, 974-975 (1995).

[50] S. Juodkazis, N. Mukai, R. Wakaki, A. Yamaguchi, S. Matsuo, and H. Misawa, "Reversible phase transitions in polymer gels induced by radiation forces," Nature **408**, 178-181 (2000).

[51] M.E. J. Friese, T.A. Nieminen, N.R. Heckenberg, and H. Rubinsztein-Dunlop, "Optical alignment and spinning of laser-trapped microscopic particles," Nature **394**, 348-350 (1998).

[52] A. La Porta and M.D. Wang, "Optical torque wrench: Angular trapping, rotation, and torque detection of quartz microparticles," Phys. Rev. Lett. **92**, 190801 (2004).

[53] M. Liu, N. Ji, Z. Lin, and S.T. Chui, "Radiation torque on a birefringent sphere caused by an electromagnetic wave," Phys. Rev. E **72**, 056610 (2005).

[54] W. Singer, T.A. Nieminen, U.J. Gibson, N.R. Heckenberg, and H. Rubinsztein-Dunlop, "Orientation of optically trapped nonspherical birefringent particles," Phys. Rev. E **73**, 021911 (2006).